Published in final edited form as:

J Immunol. 2020 July 01; 205(1): 21–25. doi:10.4049/jimmunol.2000086.

STAT1-mediated epigenetic control of *Rsad2* promotes clonal expansion of antiviral NK cells

Gabriela M. Wiedemann[1,*], **Clair Geary**[1,2,*], **Colleen M. Lau**[1,+], **Joseph C. Sun**[1,2,+]

[1]Immunology Program, Memorial Sloan Kettering Cancer Center, New York, NY, 10065

[2]Department of Immunology and Microbial Pathogenesis, Weill Cornell Medical College, New York, NY 10065

Abstract

Natural killer (NK) cells represent a cellular component of innate immunity, but possess features of adaptive immunity, including clonal expansion and establishment of long-lived memory after infection. During mouse cytomegalovirus (MCMV) infection, we observed *Rsad2* (which encodes Viperin) to be among the most highly induced interferon (IFN) stimulatory genes in activated NK cells, correlating with increased chromatin accessibility at the *Rsad2* gene loci. Furthermore, in NK cells stimulated with IFN-α, the promoter region of *Rsad2* was enriched for STAT1 binding and the permissive histone mark H3K4me3. IFNAR- and STAT1-deficient NK cells showed an impairment of *Rsad2* induction and chromatin accessibility during MCMV infection. Finally, Rsad2-deficient NK cells were defective in clonal expansion and memory formation following exposure to MCMV, in part due to greater apoptosis. Thus, our study reveals a critical mechanism of STAT1-mediated epigenetic control of *Rsad2* to promote the adaptive behavior of NK cells during viral infection.

Introduction

Although NK cells are generally considered lymphocytes of the innate immune system, recent studies in mice, humans, and non-human primates have highlighted the adaptive immune features discovered in NK cells, including the ability to undergo clonal expansion and generate memory cells (1). A subset of mouse NK cells (bearing the Ly49H receptor) and human NK cells (expressing the NKG2C receptor) recognize the viral glycoprotein m157 encoded by MCMV or HCMV-encoded peptide presented on HLA-E, respectively, and can undergo a proliferative burst (greater than 1000-fold) resulting in a long-lived pool of self-renewing memory NK cells able to be recalled (2, 3). Recent studies have demonstrated that proinflammatory cytokines (including IL-12, IL-18, and type I IFN) produced during viral infection, and signaling through downstream transcription factors

[+]Address correspondence to: Joseph C. Sun, PhD, Memorial Sloan Kettering Cancer Center, 408 East 69th Street, ZRC-1462, New York, NY 10065, Phone: 646-888-3228, Fax: 646-422-0453, sunj@mskcc.org, Colleen M. Lau, PhD, Memorial Sloan Kettering Cancer Center, 408 East 69th Street, ZRC-1425, New York, NY 10065, Phone: 646-888-3236, Fax: 646-422-0453, lauc2@mskcc.org.

[*]G.W. and C.D.G contributed equally to this work.

The authors declare no financial conflicts of interest.

(including STAT1, STAT4, Zbtb32, T-bet, Eomes, IRF8, and IRF9) can promote these adaptive NK cell processes via distinct epigenetic and transcriptional mechanisms (4–10).

During viral infection, type I IFNs are produced and bind to a heterodimeric receptor resulting in a signaling cascade leading to Janus kinase (JAK)-mediated phosphorylation and heterodimerization of signal transducer and activator of transcription 1 (STAT1) and STAT2, which complexes with IRF9 (together known as ISGF3) and translocate to the nucleus to induce the transcription of hundreds of interferon-stimulated genes (ISG) (11). Previously, we demonstrated that type I IFN via STAT1 induces a suite of genes found to promote the clonal expansion of Ly49H$^+$ NK cells following MCMV infection, involving a mechanism whereby the NK cells are shielded from apoptosis via fratricide (i.e. NK cell targeting of one another) (8). Many of the genes targeted by STAT1 in activated NK cells during virus infection have not been fully characterized.

Here, we identify *Rsad2* (which encodes Viperin) as a gene that is strongly induced in NK cells during MCMV infection. Viperin (or *virus inhibitory protein, endoplasmic reticulum-associated, interferon-inducible*) has been proposed to utilize a diverse range of mechanisms to restrict virus growth in infected host cells (12, 13). Although Rsad2/Viperin is highly conserved in evolution, it appears to have a number of functions, from being a protein that directly binds viral components, to one that regulates cholesterol biosynthesis affecting lipid rafts and virus budding, to a mediator of signaling pathways including downstream of TLRs (14–17). Viperin was recently shown to be co-opted by human CMV, where it is transported to the mitochondria and inhibits fatty acid oxidation, diminishing cellular ATP generation and leading a disruption of the actin cytoskeleton that favors the virus (18). Because the role of Rsad2/Viperin in lymphocytes is not known, we investigated mechanisms of its induction and consequences of its deletion on NK cell activation, expansion, and memory formation in response to MCMV infection.

Materials and Methods

Mice and viral infection

All mice used in this study were bred at Memorial Sloan Kettering Cancer Center in accordance with the guidelines of the Institutional Animal Care and Use Committee (IACUC). The following strains were used, all on the C57BL/6 genetic background: C57BL/6 (CD45.2), B6.SJL (CD45.1), *Ifnar1*$^{-/-}$, *Stat1*$^{-/-}$, *Irf9*$^{-/-}$, *Rsad2*$^{-/-}$ (generously provided by Dr. Peter Cresswell (Yale) (19)), *Klra8*$^{-/-}$ (*Ly49h*$^{-/-}$), NKp46-CreERT2 (20), Rosa26-lox-STOP-lox-tdTomato (21). Generation of mixed bone marrow chimeric mice (BMC) and adoptive transfer studies were performed as previously described (22). Experiments were conducted using age- and gender-matched mice in accordance with approved institutional protocols.

Naïve mice and mixed BMC mice were infected with MCMV (Smith strain) by intraperitoneal injection of 7.5×10^3 plaque-forming units (PFU). *Ly49h*$^{-/-}$ mice in adoptive transfer studies were infected with 7.5×10^2 PFU MCMV one day following NK cell transfer.

Flow cytometry and cell sorting

Single cell suspensions were prepared from indicated organs as previously described (22). Apoptosis was evaluated by using the carboxyfluorescein FLICA poly caspase assay kit (Immunochemistry Technologies) or AnnexinV assay (BD Biosciences). NK cell proliferation was analyzed by labeling cells with 5 μM Cell Trace Violet (CTV, Invitrogen) before transfer according to manufacturer's protocol. The indicated fluorophore-conjugated antibodies (Biolegend, Tonbo, eBioscience) were used to stain lymphocytes, and flow cytometry was performed on an LSR II (BD). Cell sorting was performed on an Aria II cytometer (BD). All data were analyzed with FlowJo software (TreeStar).

ChIP-Seq, RNA-seq, ATAC-seq, and bioinformatic analysis

H3K4me3 chromatin immunoprecipitation (ChIP-seq) was performed on either 1–2 × 10^5 sorted splenic NK cells (CD3ε$^-$ TCRb$^-$ CD19$^-$ F4/80$^-$ NK1.1$^+$) stimulated with or without 100 IU recombinant mouse IFN-α (R&D Systems) for 3 hours, or performed on 1–5 × 10^5 sorted Ly49H$^+$ splenic NK cells isolated during MCMV infection from WT (days 0, 2, 4, 7) or tamoxifen-treated NKp46-CreERT2 × *Rosa26*-tdTomato (tdTom$^+$; day 35 PI) mice that received 4 mg tamoxifen (Sigma) by oral gavage one day prior to infection. DNA was immunoprecipitated using 1.5 μg of rabbit polyclonal anti-H3K4me3 antibody (Millipore, 07473) and Dynabeads Protein G (Invitrogen). Illumina libraries were prepared using the KAPA HTP Library Preparation Kit (Kapa Biosystems KK8234) and HiSeq 3000/4000 SBS Kit according to the manufacturer's instructions and ran on a HiSeq 4000 in a 50bp/50bp paired end run. ChIP-seq reads from all samples were trimmed using Trimmomatic (v.0.36) then mapped to the mm10 genome using Bowtie2 (v2.2.9). Concordant mates were used for peak calling by MACS2 (v2.1.1.20160309) with arguments "–BAMPE –q 0.05". Differential analysis and count normalization was performed using DESeq2 (v1.22.2). Raw data can be found under the Gene Expression Omnibus (GEO) accession number GSE140043 (https://www.ncbi.nlm.nih.gov/geo/query/acc.cgi?acc=GSE140043).

The following datasets and analyses were performed on NK cells as previously described by our lab and can be found under the GEO accession number GSE106139 (https://www.ncbi.nlm.nih.gov/geo/query/acc.cgi?acc=GSE106139): STAT1 ChIP-seq, RNA-seq from MCMV-infected *Ifnar1*$^{-/-}$, *Stat1*$^{-/-}$, and *Irf9*$^{-/-}$ chimeras (6), RNA-seq and ATAC-seq on days 0, 2, 4, 7, 35 after MCMV infection, ATAC-seq from MCMV-infected *Stat1*$^{-/-}$ chimeras (7); RNA-seq on overnight *in vitro* cytokine stimulations (6, 10).

Statistical analyses

Data are shown as mean ± s.e.m in all graphs and statistical differences were calculated using a two-tailed unpaired Student's t-test, unless otherwise specified. P values < 0.05 were considered significant. All statistical analyses and plots were produced in GraphPad Prism or R (v3.3.3 or v3.5.3).

Results and Discussion

Potent induction of Rsad2 in NK cells during MCMV infection is dependent on IFNAR and ISGF3 components

The individual components of the ISGF3 complex (comprised of STAT1, STAT2, and IRF9) downstream of the IFN-α receptor (IFNAR) have previously been demonstrated to be critical in the generation of memory NK cells during MCMV infection (6). In RNA-seq performed on NK cells isolated from mice infected with MCMV, we observed that *Rsad2* was among the most highly induced genes between day 0 and day 2 post-infection (PI) from a list of ISGs (Fig. 1A). Just as rapidly as it was induced, *Rsad2* transcript in activated NK cells returned to near baseline by day 7 PI, and remained low in memory NK cells at day 35 PI (Fig. 1B). NK cells stimulated *ex vivo* with IFN-α, but not other pro-inflammatory cytokines, showed potent induction of *Rsad2* (Fig. 1C), consistent with previous findings performed in cell lines.

To further validate that induction of *Rsad2* in NK cells is dependent upon IFNAR signaling and ISGF3 components, we performed RNA-seq on NK cells isolated from mixed bone marrow chimeric mice generated with WT (CD45.1) and various KO (CD45.2) bones (*Ifnar1*$^{-/-}$, *Stat1*$^{-/-}$, *or Irf9*$^{-/-}$) and infected with MCMV following immune reconstitution (Fig. 1D). Whereas WT NK cells potently induced *Rsad2* transcript between day 0 and 2 PI, NK cells individually lacking IFNAR, STAT1, or IRF9 were severely impaired in *Rsad2* expression (Fig. 1E). Altogether, these data demonstrate *Rsad2* induction in NK cells early after viral infection is highly dependent on type I IFN signaling via ISGF3 components.

Rsad2 is epigenetically regulated in a STAT1-dependent manner in activated NK cells

Next we investigated how STAT1 mediates transcription of *Rsad2* in NK cells during viral infection and exposure to type I IFN. To investigate the occupancy of STAT1 across the *Rsad2* locus, we previously stimulated primary mouse NK cells with IFN-α and performed STAT1 ChIP-seq (6). Upon inspection of the *Rsad2* locus, we noticed significant STAT1 binding at the promoter region in one experimental replicate but much weaker binding in the other, providing coordinates for a putative STAT1 binding site (Fig 2A). In this second replicate, IL-2 was added to the IFN-α stimulation to improve NK cell viability and its signaling may have interfered with the ability of STAT1 to bind at the *Rsad2* promoter, as STAT5 and STAT1 can demonstrate antagonistic effects on chromatin regulation and gene transcription (Wiedemann et al, unpublished observations). To further investigate whether STAT1 affected the epigenetic regulation of *Rsad2*, we performed ChIP-seq on IFN-stimulated NK cells and observed induction of the permissive histone modification H3K4me3 at the *Rsad2* promoter in WT but not *Stat1*$^{-/-}$ NK cells (Fig. 2B). Altogether, these analyses suggest that NK cells stimulated with type I IFN induce rapid STAT1 binding and epigenetic changes at the *Rsad2* gene loci.

To investigate whether the epigenetic regulation of the *Rsad2* loci occurs during NK cell activation *in vivo*, we performed H3K4me3 ChIP-seq and ATAC-seq on Ly49H^{+} NK cells isolated at various time points PI (Fig. 2C). Interestingly, we detected a transient increase of H3K4me3 peaks (representing a ‘permissive’ histone modification) at the *Rsad2* promoter at

day 2 and 4 PI, compared to day 0 and 7 PI, which mirrored changes in chromatin accessibility (as measured by ATAC-seq) at these same time points, as demonstrated by peak 2 (Fig. 2C–E). Other peak regions followed similar patterns of maximum accessibility achieved at either day 2 PI, day 4 PI, or both (Fig. 2E). Because *Rsad2* mRNA levels were also elevated at day 2 and 4 PI (compared to day 0 and 7 PI), this indicates a transient 'permissiveness' of transcription at the *Rsad2* gene loci. In contrast, when we performed ATAC-seq on STAT1-deficient NK cells at day 2 PI, we found that the increase in chromatin accessibility was largely reduced (Fig. 2F–G), further suggesting that the transcription factor STAT1 may be actively shaping the epigenetic landscape at this ISG loci in NK cells during their activation and differentiation.

Rsad2 is essential for anti-viral NK cell expansion and survival

Given the enrichment of STAT1 and H3K4me3, and the increased chromatin accessibility at the TSS of *Rsad2* in NK cells activated during MCMV infection *in vivo*, and that *Rsad2* mRNA is strongly upregulated after viral infection, we investigated whether Rsad2 plays a role in NK cell effector function during MCMV infection. Using Rsad2-deficient mice, we first determined whether there were any defects in NK cell development or homeostasis. Consistent with its lack of expression in resting NK cells, no phenotypic or functional defects were observed in NK cells at steady state (Supplemental Fig. 1A). However, during MCMV infection, we found that *Rsad2*$^{-/-}$ NK cells (CD45.2) showed a significant defect in clonal expansion and memory compared to WT NK cells (CD45.1) co-transferred into Ly49H-deficient mice (Fig. 3A). In this adoptive transfer setting, *Rsad2*$^{-/-}$ NK cells were unable to compete with WT NK cell numbers in all organs analyzed both at early and late time points (Fig. 3B), suggesting the expansion defect of the *Rsad2*$^{-/-}$ NK cells was not a result of aberrant homing to tissues.

Finally, we assessed whether the difference in expansion between WT and *Rsad2*$^{-/-}$ NK cells could be due to differences in proliferation or survival of effector cells. We observed no difference in the expression of markers of maturation, proliferation, or cytotoxicity on day 2 after MCMV infection (Supplemental Fig. 1B). Furthermore, following CTV-labeling of both populations and transfer into MCMV-infected recipients, we observed similar rates of proliferation measured by peaks of diluted CTV (Fig. 3C), suggesting that the ability of NK cells to enter cell cycle and replicate was not impacted by loss of Rsad2. In contrast, when we stained activated NK cells using FLICA (which binds cleaved caspases as a measure of apoptosis) or AnnexinV (which binds phosphatidylserine on the outer membrane of apoptotic cells), *Rsad2*$^{-/-}$ NK cells tended to show a greater degree of FLICA incorporation or AnnexinV staining, compared to WT NK cells (Fig. 3D and data not shown). We have found that the ability to detect dying NK cells is technically challenging, as apoptotic NK cells are likely engulfed and cleared by macrophages in a rapid manner *in vivo* (23). Because the rapid clearance of dying cells is known to limit their appearance within tissues (23), we only observed the phenotype in 2 out of 3 experiments, and only in liver NK cells. Taken together, these findings suggest that type I IFN and STAT1-mediated induction of Rsad2 is essential in the clonal expansion of virus-specific NK cells, perhaps by shielding peripheral NK cells from apoptosis during their adaptive responses.

Here, we have discovered a novel and cell-intrinsic role for Rsad2 in driving the adaptive NK cell response during MCMV infection. Several previous studies have demonstrated that type I IFN and STAT1 signaling can shield different effector lymphocytes from NK cell-mediated cytotoxicity during viral infection (8, 24, 25). However, the question remained - which are the critical ISGs induced by STAT1? Consistent with our findings in NK cells lacking IFNAR, STAT1, or IRF9, where KO NK cells have a higher rate of apoptosis due to fratricide (8), we identify Rsad2 as an ISG that may be playing a role in preserving the integrity of NK cells during activation and proliferative bursts. Through epigenomic experiments, our study also highlights how STAT1 may be mediating changes in chromatin accessibility and permissiveness at the *Rsad2* loci to promote its transcription. These findings are consistent with recent studies highlighting such a chromatin-modifying and epigenetic mechanism for STAT transcription factors, in particular data demonstrating that proinflammatory IL-12 signaling in activated NK cells initiates STAT4 nuclear translocation and binding to regulatory gene regions, induction of chromatin accessibility changes, and subsequent transcription at specific gene loci (e.g. *Irf8, Zbtb32*, *Runx1*, and *Runx3*) (4, 5, 10).

Given that the role for Rsad2 in many biological processes is quite broad (26), and that it can associate with mitochondria to influence cellular metabolism (17), it is perhaps unsurprising that our data highlights a novel role for this protein in mediating NK cell survival versus death during rapid proliferation. Nonetheless, we have identified and implicated the first ISG in these adaptive NK cell responses during infection. Future mechanistic studies are required to determine precisely how Rsad2 is mediating its protective role in rapidly dividing NK cells, with the ultimate goal of being able to harness or enhance potent NK cell responses against infectious diseases and cancer.

Supplementary Material

Refer to Web version on PubMed Central for supplementary material.

Acknowledgments

G.M.W. was supported by a DFG fellowship (DFG Forschungsstipendium WI-4927/1). C.M.L. was supported by the Cancer Research Institute as a Cancer Research Institute-Carson Family Fellow. J.C.S. was supported by the Ludwig Center for Cancer Immunotherapy, the American Cancer Society, the Burroughs Wellcome Fund, and the NIH (AI100874, AI130043, and P30CA008748).

References

1. O'Sullivan TE, Sun JC, and Lanier LL. 2015 Natural Killer Cell Memory. Immunity 43: 634–645. [PubMed: 26488815]
2. Rapp M, Wiedemann GM, and Sun JC. 2018 Memory responses of innate lymphocytes and parallels with T cells. Semin. Immunopathol 40: 343–355. [PubMed: 29808388]
3. Sun JC, Beilke JN, and Lanier LL. 2009 Adaptive immune features of natural killer cells. Nature 457: 557–561. [PubMed: 19136945]
4. Adams NM, Lau CM, Fan X, Rapp M, Geary CD, Weizman OE, Diaz-Salazar C, and Sun JC. 2018 Transcription Factor IRF8 Orchestrates the Adaptive Natural Killer Cell Response. Immunity 48: 1172–1182 e1176. [PubMed: 29858012]

5. Beaulieu AM, Zawislak CL, Nakayama T, and Sun JC. 2014 The transcription factor Zbtb32 controls the proliferative burst of virus-specific natural killer cells responding to infection. Nat. Immunol 15: 546–553. [PubMed: 24747678]
6. Geary CD, Krishna C, Lau CM, Adams NM, Gearty SV, Pritykin Y, Thomsen AR, Leslie CS, and Sun JC. 2018 Non-redundant ISGF3 Components Promote NK Cell Survival in an Auto-regulatory Manner during Viral Infection. Cell. Rep 24: 1949–1957 e1946. [PubMed: 30134157]
7. Lau CM, Adams NM, Geary CD, Weizman OE, Rapp M, Pritykin Y, Leslie CS, and Sun JC. 2018 Epigenetic control of innate and adaptive immune memory. Nat. Immunol 19: 963–972. [PubMed: 30082830]
8. Madera S, Rapp M, Firth MA, Beilke JN, Lanier LL, and Sun JC. 2016 Type I IFN promotes NK cell expansion during viral infection by protecting NK cells against fratricide. J. Exp. Med 213: 225–233. [PubMed: 26755706]
9. Madera S, and Sun JC. 2015 Cutting edge: stage-specific requirement of IL-18 for antiviral NK cell expansion. J. Immunol 194: 1408–1412. [PubMed: 25589075]
10. Rapp M, Lau CM, Adams NM, Weizman OE, O'Sullivan TE, Geary CD, and Sun JC. 2017 Core-binding factor beta and Runx transcription factors promote adaptive natural killer cell responses. Sci. Immunol 2: eaan3796. [PubMed: 29222089]
11. Ivashkiv LB, and Donlin LT. 2014 Regulation of type I interferon responses. Nat. Rev. Immunol 14: 36–49. [PubMed: 24362405]
12. Chin KC, and Cresswell P. 2001 Viperin (cig5), an IFN-inducible antiviral protein directly induced by human cytomegalovirus. Proc. Natl. Acad. Sci. USA 98: 15125–15130. [PubMed: 11752458]
13. Seo JY, Yaneva R, and Cresswell P. 2011 Viperin: a multifunctional, interferon-inducible protein that regulates virus replication. Cell Host Microbe 10: 534–539. [PubMed: 22177558]
14. Wang X, Hinson ER, and Cresswell P. 2007 The interferon-inducible protein viperin inhibits influenza virus release by perturbing lipid rafts. Cell Host Microbe 2: 96–105. [PubMed: 18005724]
15. Saitoh T, Satoh T, Yamamoto N, Uematsu S, Takeuchi O, Kawai T, and Akira S. 2011 Antiviral protein Viperin promotes Toll-like receptor 7- and Toll-like receptor 9-mediated type I interferon production in plasmacytoid dendritic cells. Immunity 34: 352–363. [PubMed: 21435586]
16. Rivieccio MA, Suh HS, Zhao Y, Zhao ML, Chin KC, Lee SC, and Brosnan CF. 2006 TLR3 ligation activates an antiviral response in human fetal astrocytes: a role for viperin/cig5. J. Immunol 177: 4735–4741. [PubMed: 16982913]
17. Seo JY, and Cresswell P. 2013 Viperin regulates cellular lipid metabolism during human cytomegalovirus infection. PLoS Pathog. 9: e1003497. [PubMed: 23935494]
18. Seo JY, Yaneva R, Hinson ER, and Cresswell P. 2011 Human cytomegalovirus directly induces the antiviral protein viperin to enhance infectivity. Science 332: 1093–1097. [PubMed: 21527675]
19. Qiu LQ, Cresswell P, and Chin KC. 2009 Viperin is required for optimal Th2 responses and T-cell receptor-mediated activation of NF-kappaB and AP-1. Blood 113: 3520–3529. [PubMed: 19047684]
20. Nabekura T, and Lanier LL. 2016 Tracking the fate of antigen-specific versus cytokine-activated natural killer cells after cytomegalovirus infection. J. Exp. Med 213: 2745–2758. [PubMed: 27810928]
21. Madisen L, Zwingman TA, Sunkin SM, Oh SW, Zariwala HA, Gu H, Ng LL, Palmiter RD, Hawrylycz MJ, Jones AR, Lein ES, and Zeng H. 2010 A robust and high-throughput Cre reporting and characterization system for the whole mouse brain. Nat. Neurosci 13: 133–140. [PubMed: 20023653]
22. Adams NM, Geary CD, Santosa EK, Lumaquin D, Le Luduec JB, Sottile R, van der Ploeg K, Hsu J, Whitlock BM, Jackson BT, Weizman OE, Huse M, Hsu KC, and Sun JC. 2019 Cytomegalovirus Infection Drives Avidity Selection of Natural Killer Cells. Immunity 50: 1381–1390 e1385. [PubMed: 31103381]
23. Elliott MR, and Ravichandran KS. 2016 The Dynamics of Apoptotic Cell Clearance. Dev. Cell 38: 147–160. [PubMed: 27459067]

24. Crouse J, Bedenikovic G, Wiesel M, Ibberson M, Xenarios I, Von Laer D, Kalinke U, Vivier E, Jonjic S, and Oxenius A. 2014 Type I interferons protect T cells against NK cell attack mediated by the activating receptor NCR1. Immunity 40: 961–973. [PubMed: 24909889]

25. Xu HC, Grusdat M, Pandyra AA, Polz R, Huang J, Sharma P, Deenen R, Kohrer K, Rahbar R, Diefenbach A, Gibbert K, Lohning M, Hocker L, Waibler Z, Haussinger D, Mak TW, Ohashi PS, Lang KS, and Lang PA. 2014 Type I interferon protects antiviral CD8+ T cells from NK cell cytotoxicity. Immunity 40: 949–960. [PubMed: 24909887]

26. Helbig KJ, and Beard MR. 2014 The role of viperin in the innate antiviral response. J. Mol. Biol 426: 1210–1219. [PubMed: 24157441]

Key Points

- Type I IFN potently upregulates *Rsad2* mRNA in NK cells
- *Rsad2* is epigenetically and transcriptionally regulated by STAT1
- Rsad2 contributes to NK cell clonal expansion and memory formation during infection

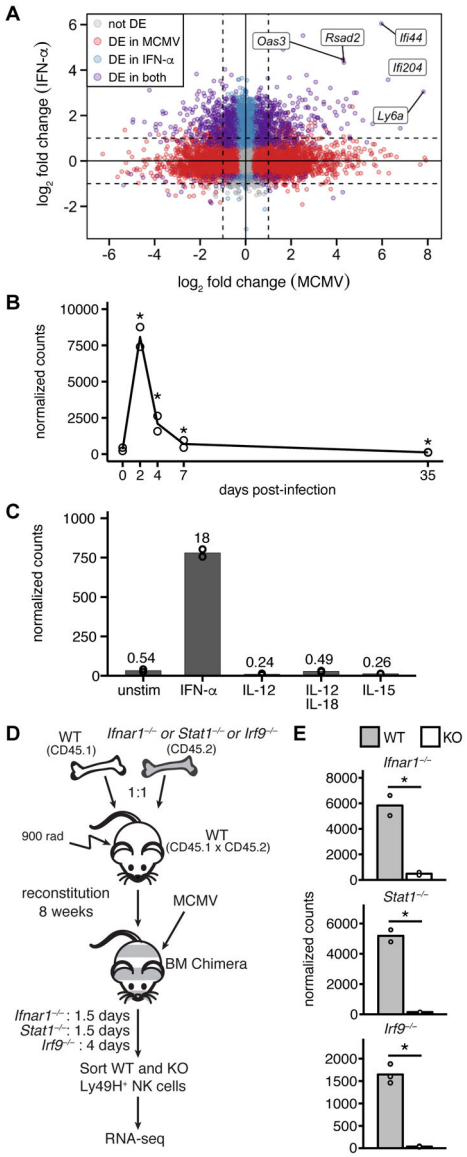

Fig. 1. Induction of *Rsad2* expression in NK cells is dependent on type I IFN signaling *in vitro* and *in vivo.*

(**A**) Scatter plots of RNA-seq $\log_2$ FC comparing Ly49H$^+$ NK cells at d2 following MCMV infection versus d0 (x-axis) to IFN-α-stimulated NK cells versus unstimulated *in vitro* (y-axis). Red, blue and purple dots indicate genes that were DE (FDR-adjusted p-value < 0.05) only in MCMV infection, only IFN-α-stimulated, or both, respectively. Top 5 genes ranked on average FC among common DE genes are highlighted. (**B**) RNA-seq normalized counts of *Rsad2* from MCMV-infected Ly49H$^+$ NK cells at indicated days PI. Asterisks indicate DE compared to d0. (**C**) RNA-seq normalized counts of *Rsad2* from sorted NK cells stimulated with various cytokines for 16 hrs. Numbers above bars display transcript abundance as average TPM. (**D**) Experimental schematic of mixed BMC prepared for RNA-seq following infection. (**E**) RNA-seq normalized counts of *Rsad2* from Ly49H$^+$ NK cells from BMCs described in (D). All barplots and lines show mean.

FC=fold change, PI=post-infection, DE=differentially expressed, TPM=transcripts-per-million

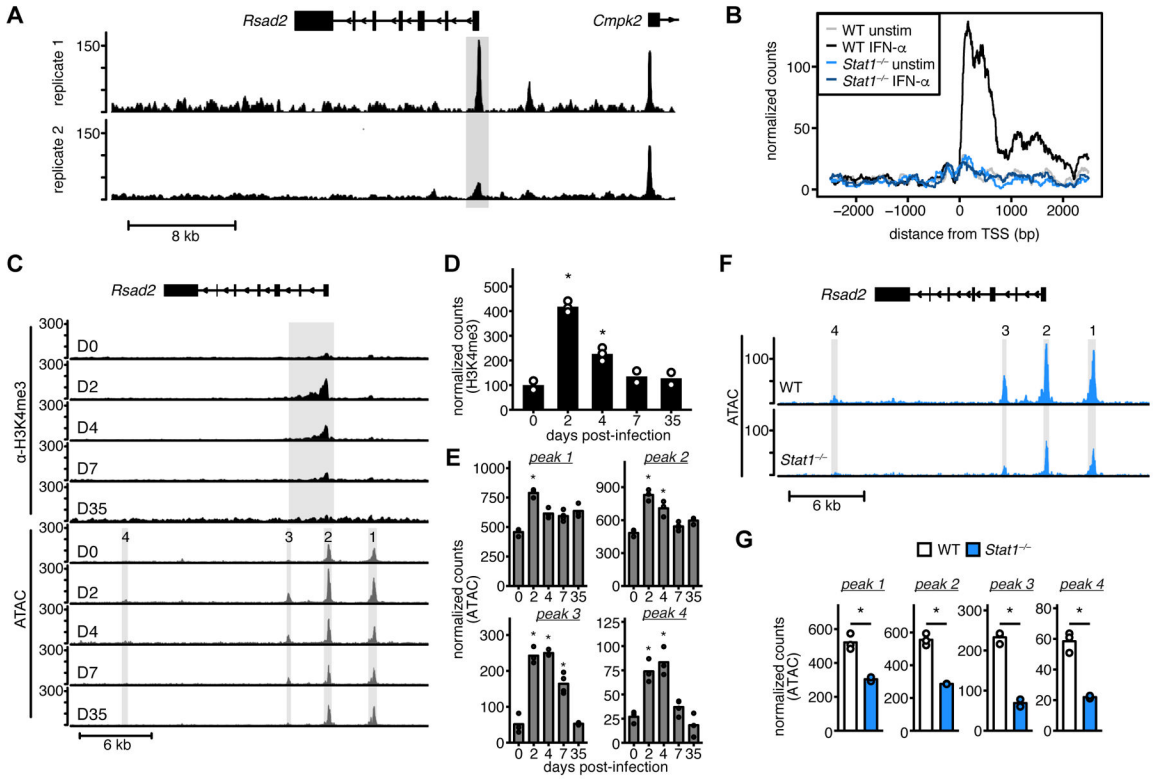

Fig. 2. *Rsad2* is epigenetically regulated by STAT1.

(**A**) ChIP-seq gene tracks show STAT1 signal as normalized fragment pileup (y-axis) plotted by genome position (x-axis) from IFN-α-stimulated NK cells. Shaded box highlights putative STAT1 binding site at the *Rsad2* promoter region. (**B**) Line plots depict normalized count coverage of H3K4me3 signal in unstimulated and IFN-α-stimulated NK cells isolated from WT or *Stat1*$^{-/-}$ mice. (**C**) Ly49H^{+} NK cells were harvested at indicated time points after MCMV infection and processed for ChIP-seq and ATAC-seq. Gene tracks show H3K4me3 ChIP-seq signal as normalized fragment pileup (top rows; black) and chromatin accessibility (bottom rows; gray) as normalized reads (y-axis), both plotted by genome position (x-axis). Shaded boxes highlight differentially modified or accessible peak regions. (**D**) Total normalized counts within H3K4me3 peak region highlighted in (C). (**E**) Total normalized counts within ATAC peak regions highlighted in (C). (**F**) Gene tracks show chromatin accessibility as in (C) from Ly49H^{+} NK cells harvested at day 2 PI from WT:*Stat1*$^{-/-}$ mixed BMC as shown in Fig. 1D. (**G**) Total normalized counts within ATAC peak regions highlighted in (F). * FDR-adjusted p-value < 0.05

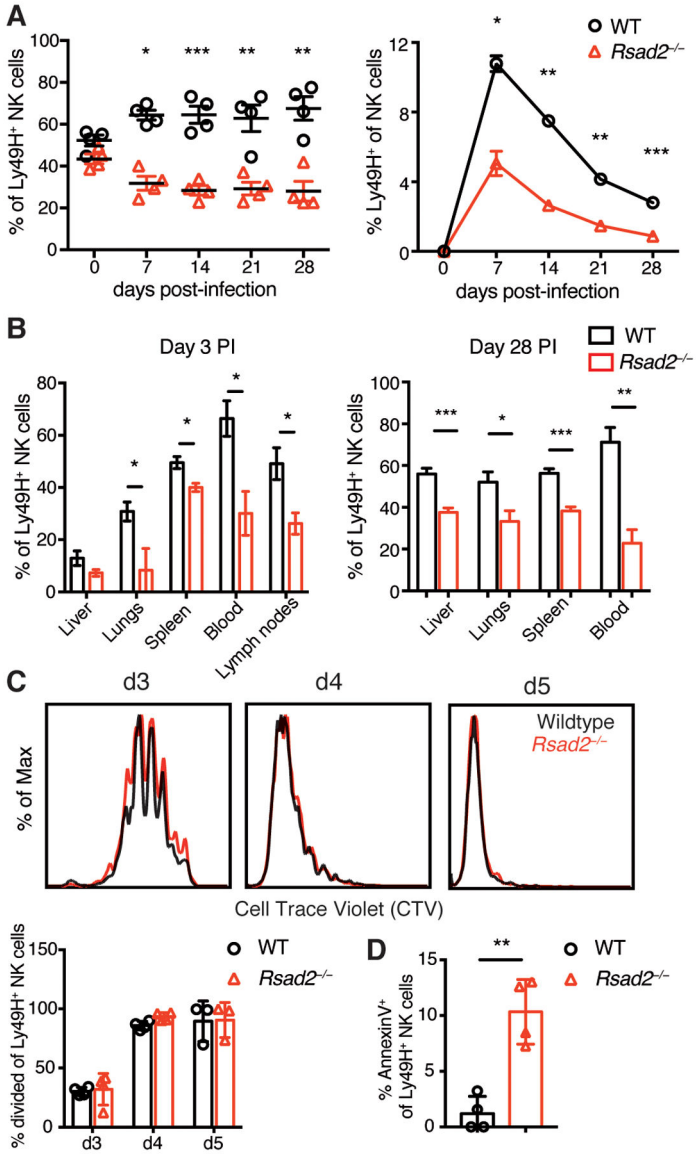

Fig. 3. *Rsad2* is required for NK cell expansion and memory formation.

(A) Splenocytes from WT:*Rsad2*$^{-/-}$ mixed BMC where adoptively transferred into *Ly49h*$^{-/-}$ mice, followed by infection with MCMV. Percentage of NK cells in each group were calculated at each time point over the course of the infection. Graphs show the percentage of the two populations within the transferred Ly49H^{+} cells (left) and within total NK cells of the recipient (right). (**B**) Graphs show the percentages of WT and *Rsad2*$^{-/-}$ NK cells within the total Ly49H^{+} population in different organs on days 3 and 28 PI. Data is representative of 2 independent experiments (n=4–5). (**C**) WT or *Rsad2*$^{-/-}$ NK cells were stained with CTV and transferred into *Ly49h*$^{-/-}$ mice, followed by infection with MCMV. Spleens and livers were analyzed on day 3, 4 and 5 PI, and representative histograms and graph show percentages of divided WT and *Rsad2*$^{-/-}$ NK cells. Data is representative of 3 independent experiments (n =4–5). (**D**) WT or *Rsad2*$^{-/-}$ NK cells were transferred into *Ly49h*$^{-/-}$ mice,

followed by infection with MCMV. Graph shows the percentage of AnnexinV^{+} cells within each transferred group on day 3 PI in the liver (n = 4).